

Ultra-low-noise tunnel junction dc SQUID with a tightly coupled planar input coil

M. B. Ketchen and J. M. Jaycox

Citation: [Applied Physics Letters](#) **40**, 736 (1982); doi: 10.1063/1.93210

View online: <http://dx.doi.org/10.1063/1.93210>

View Table of Contents: <http://scitation.aip.org/content/aip/journal/apl/40/8?ver=pdfcov>

Published by the [AIP Publishing](#)

Articles you may be interested in

[Very low noise, tightly coupled, dc SQUID amplifiers](#)

Appl. Phys. Lett. **49**, 1118 (1986); 10.1063/1.97440

[Resistively shunted dc SQUID coupled to an input coil](#)

J. Appl. Phys. **59**, 1714 (1986); 10.1063/1.336436

[Low noise niobium dc SQUID with a planar input coil](#)

Appl. Phys. Lett. **42**, 389 (1983); 10.1063/1.93917

[Low-noise tunnel junction dc SQUID's](#)

Appl. Phys. Lett. **38**, 723 (1981); 10.1063/1.92472

[An ultra-low-noise tunnel junction dc SQUID](#)

Appl. Phys. Lett. **35**, 812 (1979); 10.1063/1.90946

This is a promotional banner for Applied Physics Reviews. On the left, there is a small image of the journal's cover, which features a diagram of a device. The main part of the banner has a blue background with a bright light source on the right. The text "NEW Special Topic Sections" is prominently displayed in white. Below this, on an orange background, it says "NOW ONLINE" in yellow, followed by "Lithium Niobate Properties and Applications: Reviews of Emerging Trends" in white. The AIP Applied Physics Reviews logo is in the bottom right corner.

NEW Special Topic Sections

NOW ONLINE
Lithium Niobate Properties and Applications:
Reviews of Emerging Trends

AIP Applied Physics Reviews

Ultra-low-noise tunnel junction dc SQUID with a tightly coupled planar input coil

M. B. Ketchen and J. M. Jaycox^{a)}

IBM Thomas J. Watson Research Center, Yorktown Heights, New York 10598

(Received 2 December 1981; accepted for publication 26 January 1982)

We present a new superconducting quantum interference device (SQUID) that combines ultra-low-noise performance with tight coupling to a useable input coil. The inductive loop of the SQUID consists of a superconducting square washer that is slit in a low inductance fashion from its central hole to an outside edge where two Josephson tunnel junctions are incorporated. The inductance of the SQUID is about 90 pH, and each junction has a critical current of 15 μ A and a resistive shunt of 4.5 Ω . The 190-nH input coil is a planar spiral of 50 turns situated immediately above the washer and coupled to the SQUID with a coupling constant k^2 of 0.86. The SQUID has a minimum coupled energy sensitivity of $19h$ at 4.2 K and $8h$ at 1.5 K, in good agreement with theory. The crossover between white and low frequency noise occurs at ~ 250 Hz.

PACS numbers: 85.25. + k, 74.50. + r

The figure of merit used to characterize the performance of a superconducting quantum interference device (SQUID) is given by the coupled energy sensitivity $\epsilon^c = \phi_n^2 / 2k^2 L$, where ϕ_n is the rms flux noise per Hz^{1/2}, L is the self-inductance of the SQUID, and k^2 is the coupling constant between the SQUID and its input coil.^{1,2} The input coil should be of sufficiently high self-inductance to allow efficient matching to circuits of interest, typically ~ 100 –2000 nH. A number of workers have recently reported dc SQUID's of planar geometry having values of intrinsic energy sensitivity, $\epsilon = \phi_n^2 / 2L$, approaching the quantum limit of $\sim h$.^{3–7} These results are very significant; however, for practical applications it is the *coupled* energy sensitivity that is important. While recent low noise dc SQUID's have all been planar thin-film designs, high performance, well coupled SQUID's have traditionally been cylindrical⁸ or toroidal⁹ in geometry. A notable exception is the fractional turn planar SQUID of Cromar and Carelli⁶ which with $\epsilon^c = 71h$ for a 1600-nH input coil outperformed all previously reported dc SQUID's. In this letter we describe a planar SQUID with a tightly coupled 190-nH input coil that has a minimum coupled energy sensitivity of $8h$. The design is directly extendable to input coil inductances anywhere in the range of 10–2000 nH and to noise performance approaching the quantum limit.

The SQUID consists of an 89-pH superconducting loop interrupted by two 2- μ m-diam Josephson junctions, each of critical current $I_0 \approx 15 \mu$ A. The junctions are individually shunted by a discrete resistance $R \approx 4.5 \Omega$ and by self and parasitic capacitance $C \approx 0.3$ pF. The hysteresis parameter $\beta_c = 2\pi I_0 R^2 C / \phi_0$ (ϕ_0 is the flux quantum) is about 0.3 so that the junctions are nonhysteretic.^{10,11} There is a capacitance $C_L \gg C$ that divides the inductive loop into two meshes, making this a double loop SQUID.¹² According to Tesche the traditional theory for noise in dc SQUID's¹³ should hold provided the device is biased with a gate current $I_B > 2I_0$. For $I_B < 2I_0$ a new kind of hysteretic behavior is predicted which would lead to very high noise levels.¹² Traditional

theory predicts that in the thermal limit with $\beta = 2LI_0\phi_0^{-1} \approx 1$ this SQUID should have a minimum coupled energy sensitivity in the white noise region given by^{13,14}

$$\epsilon_w^c = \frac{\gamma h}{k^2} \frac{k_B T}{e I_0 R} \approx h \left(\frac{5.5\gamma}{k^2} \right) \left(\frac{T}{4.2 \text{ K}} \right), \quad (1)$$

where the parameter γ is in the range of 2–5. The value of $I_0 R \approx 65 \mu$ V was chosen to be consistent with fabrication capability¹⁵ and to give β_c well below unity. Smaller, higher current density junctions would permit at least an order of magnitude increase in $I_0 R$, bringing ϵ_w^c to $\sim h$ at 1–2 K.¹⁴

The $1/f$ noise in dc SQUID's is not well understood. One theory that does roughly agree with existing data for ultra-low-noise SQUID's is based on a semiempirical thermal fluctuation model.^{16,17} This theory, which assumes a $1/f$ spectrum, predicts a crossover between white noise and low-frequency noise in a SQUID with $\beta \approx 1$ at a characteristic frequency f_0 given by¹⁸

$$f_0 \approx \frac{T(I_0 R)^3}{4\gamma \mathcal{H} \phi_0 \beta_c} \left(\frac{d\beta}{dT} \right)^2, \quad (2)$$

where \mathcal{H} is the ratio of the heat capacity of the thermal volume of the junction¹⁷ to the junction capacitance. For the present SQUID fabricated with a Pb alloy technology^{15,18} we estimate $f_0 \approx 500\gamma^{-1}$ Hz at 4.2 K.

Our SQUID makes use of an efficient planar coupling scheme.¹⁹ The inductive loop of the SQUID consists of a superconducting square washer as shown in Fig. 1(a). The overlapping slit configuration which makes a contribution of ~ 5 pF to C_L provides a low inductance path from the hole region of the washer, near which currents tend to flow, to the two Josephson junctions remotely located at an outside edge of the washer. The inductance of the SQUID is dominated by that of the washer which from numerical calculations^{20,21} is given by¹⁹ $L_w \approx 1.25 \mu_0 d$, where d is the distance across the hole. The input coil [shown as a simplified two-turn version in Fig. 1(a)] is fabricated as a planar spiral insulated from the washer directly below. The line from the center of the coil to its outside edge is on a separate level insulated from both the spiral and the washer. In the same way the quarter-turn

^{a)}Present address: Texas Instruments, P. O. Box 225621 M/S 964, Dallas, Texas 75222.

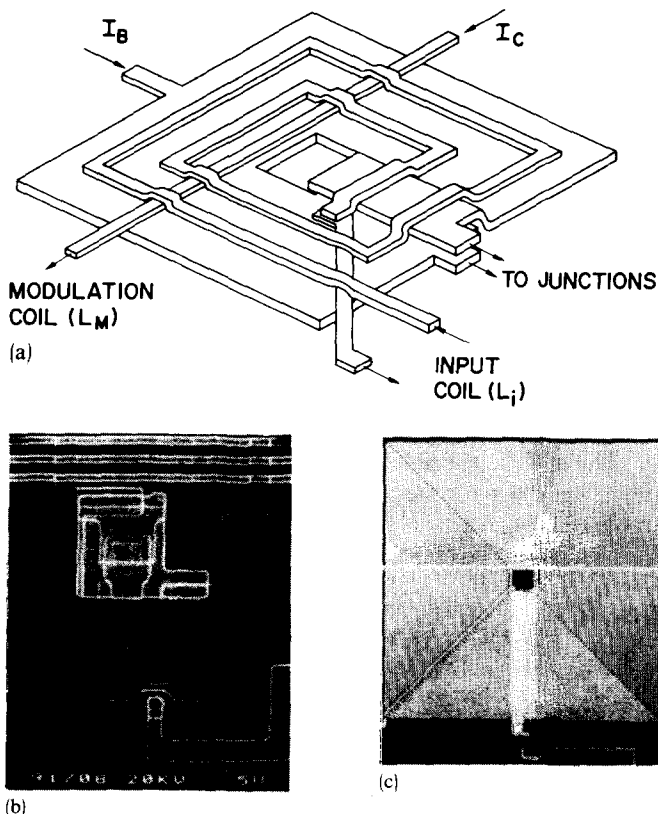


FIG. 1. (a) Square washer SQUID inductance design with spiral input coil and quarter-turn modulation coil, (b) micrograph of the junction region of the SQUID, and (c) micrograph of the entire SQUID with its 50-turn input coil.

modulation coil (L_M) is threaded between the spiral and washer.

A micrograph of the junction region of the SQUID and its connections to the low inductance overlap are shown in Fig. 1(b), and a micrograph of the entire SQUID is shown in Fig. 1(c). In all, 11 different levels of metallization and insulation were used to fabricate the SQUID.¹⁵ Nb is the material used for the square washer (not for the overlap) and also beneath the junction region. Except for the tunnel barrier and a thin Nb_2O_5 layer over the Nb, all insulators are SiO_2 . The other superconducting structures are Pb alloys and the resistive shunts are AuIn_2 . The physical design of the junction region is very similar to that previously described.³ Portions of the outer three turns of the input coil can be seen in the upper part of Fig. 1(b). The two circular window junctions are located just below the center of that figure. The distance across the inner hole of the washer [Fig. 1(c)] is about $50\text{ }\mu\text{m}$, while the outside dimension is about 0.7 mm . The spiral consists of 50 turns of $2.5\text{-}\mu\text{m}$ -wide line on a $6.25\text{-}\mu\text{m}$ pitch. The input coil inductance as determined by an inductive split experiment is about 190 nH ; the self-inductance of the SQUID from modulation depth measurements is about 89 pH ; the mutual inductance between the input coil and SQUID is 3.8 nH , and $k^2 \approx 0.86$.¹⁹ A redesign for a higher value of L_i requires only that one expand the outer dimension of the square washer to a size that will accommodate the desired number of input coil turns, while keeping the same central hole size and junction region design. Under such a

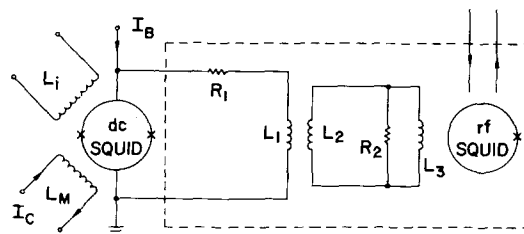


FIG. 2. Diagram of the rf SQUID readout scheme. The circuit within the dotted line acts as a low-noise preamplifier to read out the dc SQUID.

transformation L , dominated by L_w , will remain nearly constant, M_i will increase linearly with n , and L_i will increase as n^2 . This behavior has been experimentally verified for $10\text{ nH} \leq L_i \leq 800\text{ nH}$ and should continue to hold to values of L_i of at least several μH .¹⁹

The noise performance of the dc SQUID was evaluated using an rf SQUID²² readout scheme,¹⁸ the circuit diagram of which is shown in Fig. 2. The input coil (L_3) of the rf SQUID is shunted by a resistor ($R_2 \approx 3\text{ }\Omega$) to reduce high-frequency noise fed into the rf SQUID. A superconducting wire wound intermediate transformer (L_1 and L_2) provides a measured current gain of 5.2. The standard resistor R_1 has a value of $\sim 9.5\text{ }\Omega$. The dynamic resistance of the dc SQUID in regions where the noise was measured was typically $2\text{--}3\text{ }\Omega$, so that the rf SQUID system acted as a low noise, high impedance preamplifier. The frequency response of the system is flat to within $\pm 10\%$ out to about 5 kHz . All noise voltage data were multiplied by the measured 4.2- or 1.5-K frequency response which was normalized to the system gain at dc. For noise measurements the SQUID bias current I_B and control current I_C [Figs. 1(a) and 2] are supplied by Hg battery sources. The dc SQUID, standard resistor, and intermediate transformer are located within a Pb shield; the rf SQUID with its input coil and R_2 are in a separate Nb shield.²² A twisted pair of superconducting wires threaded through a Nb capillary connects the intermediate transformer to the input coil of the rf SQUID. With the dc SQUID in the superconducting state, the noise of the system is dominated by the thermal noise of the standard resistor. In separate experiments the I_B and I_C sources were connected directly to the input of the intermediate transformer with the dc SQUID removed. At current levels 3–10 times those used for the SQUID noise measurements, no excess noise was observed above 1 Hz . With the dc SQUID biased in regions of good noise performance, the system noise is dominated by that of the dc SQUID, although the standard resistor continues to make a non-negligible contribution (typically $\sim 30\%$ of the total noise power in the white noise region). The technique employed for background subtraction was to assume that all of the background noise originates in R_1 . Compared to what is present when the dc SQUID is superconducting, the voltage noise power associated with R_1 that appears at the output of the rf SQUID electronics is reduced by a factor of $\eta^2 = [R_1/(R_1 + R_D)]^2$ when the dc SQUID is biased in the voltage state with a dynamic resistance R_D . The noise present with the dc SQUID superconducting multiplied by η^2 gives a conservative estimate of the background since only the noise from R_1 and not that from R_2 or the rf SQUID is

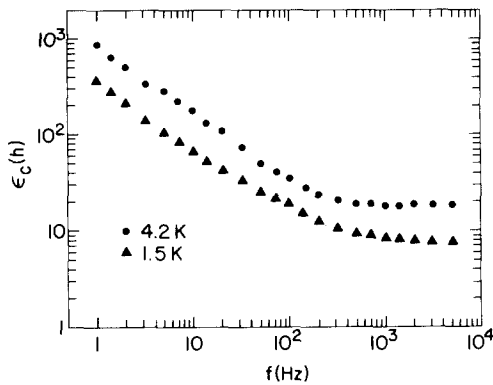


FIG. 3. Coupled energy sensitivity ϵ^c as a function of frequency f at 4.2 and 1.5 K.

actually reduced by η^2 . The quantity $1-\eta$, a current divider relation, can be directly determined by measuring the fraction of a small change in bias current that passes through L_1 .

To evaluate the flux noise ϕ_n one first introduces a small change ($\Delta\phi \sim 10^{-4} \phi_0$) in the quasistatic flux applied to the SQUID by making a calibrated change in I_C . The accompanying change in the room-temperature output voltage of the rf SQUID electronics is measured and then divided by $\Delta\phi$ to get $\partial V/\partial\phi$. At the same dc SQUID bias point the voltage noise V_n at the output of the rf SQUID system is measured from 1 Hz to 5 kHz. V_n is then multiplied by the normalized rf SQUID system transfer function, squared, and corrected for background (using the value of η^2 for that particular dc SQUID bias point). The resulting voltage noise power spectrum divided by $2(\partial V/\partial\phi)^2 k^2 L$ gives ϵ^c .

Figure 3 shows representative ϵ^c curves measured with the input coil open and the SQUID immersed in liquid helium at 4.2 and 1.5 K. The minimum value of ϵ^c in the white noise region was found to be $19h$ at 4.2 K and $8h$ at 1.5 K. These data are in good agreement with Eq. (1) for $\gamma \approx 3.3$. The crossover frequency f_0 between the low frequency and white noise is within a factor of 2 of the 150 Hz predicted by Eq. (2) although the low-frequency noise varies as $f^{-0.7}$ rather than f^{-1} as was assumed in the original derivation of Eq. (2). The value of I_B at which these data were taken was $\sim 1.5(2I_0)$ where the SQUID parameters took on values consistent with those assumed for the derivation of Eq. (1). While the very best noise performance was fairly localized in applied flux ($\sim 10^{-2} \phi_0$), good performance could be obtained over a considerably wider range. For example at 1.5 K a region was found $\sim 0.15\phi_0$ in width having a minimum ϵ_w^c

of $8h$, but with ϵ_w^c everywhere less than $25h$. There were also regions with $I_B > 2I_0$ where the SQUID was considerably noisier than the simple theory predicts. In addition with $I_B \lesssim 2I_0$ the SQUID, when in the voltage state, was extremely noisy at all bias points, consistent with recent predictions of Tesche for the double loop SQUID.¹²

In summary we have demonstrated that the planar dc SQUID shown in Figs. 1(a)–1(c) has very low-noise performance as well as excellent coupling characteristics. With $\epsilon_w^c \approx 8h$ and $L_i \approx 190$ nH this SQUID shows considerable promise for use in experimental applications. The design is flexible in that it allows a wide variation of L_i with minimal redesign effort, as well as further improvements in ϵ_w^c for an increase in $I_0 R$.

The authors are indebted to J. Greiner and his circuit fabrication group for their expert preparation of the SQUID samples. M. Naor assisted with the characterization of the rf SQUID readout system and with noise measurements.

¹V. Radhakrishnan and V. L. Newhouse, J. Appl. Phys. **42**, 129 (1971).

²J. H. Claassen, J. Appl. Phys. **46**, 2268 (1975).

³M. B. Ketchen and R. F. Voss, Appl. Phys. Lett. **35**, 812 (1979).

⁴R. F. Voss, R. Laibowitz, and A. N. Broers, Appl. Phys. Lett. **37**, 656 (1980).

⁵R. F. Voss, R. B. Laibowitz, A. N. Broers, S. I. Raider, C. M. Knoedler, and J. M. Viggiano, IEEE Trans. Magn. **MAG-17**, 395 (1981).

⁶M. W. Cromar and P. Carelli, Appl. Phys. Lett. **38**, 723 (1981).

⁷D. J. Van Harlingen, R. H. Koch, and J. Clarke, Physica **108B + C**, Nos. 1–3, 1083 (1981).

⁸J. Clarke, W. M. Goubau, and M. B. Ketchen, J. Low Temp. Phys. **25**, 99 (1976).

⁹R. P. Giffard, R. A. Webb, and J. C. Wheatley, J. Low Temp. Phys. **6**, 533 (1972).

¹⁰W. C. Stewart, Appl. Phys. Lett. **12**, 277 (1968).

¹¹D. E. McCumber, J. Appl. Phys. **39**, 3113 (1968).

¹²C. D. Tesche, J. Low Temp. Phys. (in press).

¹³C. D. Tesche and J. Clarke, J. Low Temp. Phys. **29**, 301 (1977).

¹⁴M. B. Ketchen, IEEE Trans. Magn. **MAG-17**, 387 (1981).

¹⁵J. H. Greiner, C. J. Kircher, S. P. Klepner, S. K. Lahiri, A. J. Warnecke, S. Basavaiah, E. T. Wen, John M. Baker, P. R. Brosious, H. C. W. Huang, M. Murakami, and I. Ames, IBM J. Res. Dev. **24**, 195 (1980).

¹⁶Richard F. Voss and John Clarke, Phys. Rev. B **13**, 556 (1976).

¹⁷J. Clarke and G. A. Hawkins, IEEE Trans. Magn. **MAG-11**, 841 (1975).

¹⁸M. B. Ketchen and C. C. Tsuei, in *SQUID '80*, edited by H.-D. H. Hahlbohm and H. Lubbig (Walter de Gruyter, Berlin, New York, 1980), p. 227.

¹⁹J. M. Jaycox and M. B. Ketchen, IEEE Trans. Magn. **MAG-17**, 400 (1981).

²⁰W. H. Chang, IEEE Trans. Magn. **MAG-17**, 764 (1981).

²¹W. H. Chang, a three-dimensional version of technique described in Ref. 20 (private communication).

²²The rf SQUID used was a S.H.E. Model 300X.